

# Microstructure and mechanical properties of 3D-printed dental Co-Cr alloys, produced with the use of selective laser melting

SABINA CHERNEVA<sup>1\*</sup>, VLADIMIR PETRUNOV<sup>2</sup>, VLADIMIR PETKOV<sup>3</sup>,  
VLADIMIR BOGDANOV<sup>2</sup>, SILVIYA SIMEONOVA<sup>4</sup>

<sup>1</sup> Institute of Mechanics, Bulgarian Academy of Sciences, Bulgaria.

<sup>2</sup> Faculty of Dental Medicine, Medical University of Sofia, Sofia, Bulgaria.

<sup>3</sup> Institute of Metal Science, Equipment and Technologies with Hydro- and Aerodynamics Centre,  
“Acad. A. Balevski”, Bulgarian Academy of Sciences, Bulgaria.

<sup>4</sup> Faculty of Chemistry and Pharmacy, Sofia University, Sofia, Bulgaria.

*Purpose:* The aim of present work was to investigate microstructure and mechanical properties of 3D printed by selective laser melting (SLM) Co-Cr alloys, intended for additive manufacturing in dentistry. *Methods:* A scanning electron microscope (SEM), equipped with an integrated Energy-Dispersive X-Ray Spectroscopy (EDS) system was used for investigation of the surface morphology and elemental composition of the 3D-printed Co-Cr sample. The X-ray structural analysis of the 3D-printed Co-Cr sample was made with a Bruker D8 Advance powder X-ray diffractometer. An atomic force microscopy (AFM) was used to investigate the surface topography of the sample. Tensile test, a three-point bending test and nanoindentation experiments were conducted for investigation of mechanical properties of the 3D-printed Co-Cr sample. The influence of two different strain rates (1 mm/min and 60 mm/min) on the flexural strength was investigated as well. *Results:* Higher values of indentation hardness (6.76 GPa), tensile strength (1016 MPa), yield strength (636.5 MPa) and flexural strength (1908 and 1891 MPa) of the Co-Cr alloys produced with the use of selective laser melting have been obtained, compared to cast Co-Cr and Cr-Ni alloys. It was found that increasing the strain rate from 1 mm/min to 60 mm/min caused a proportional decrease in recorded flexural strength of ~0.9%. *Conclusions:* The obtained results showed that the laser-sintered Co-Cr alloy can fully replace the cast Co-Cr alloy in dentistry, regarding its good mechanics properties as well as the high precision of the final product.

*Key words:* 3D printing, cobalt-chromium alloys, selective laser melting, mechanical properties, surface structure, dentistry

## 1. Introduction

In modern orthodontic practice, when choosing appliances, clinicians are increasingly directed towards the composition of fixed appliances [35]. The main reason for this is that the use of fixed appliances largely excludes the factor of patient cooperation. It is a proven fact that the level of cooperation among orthodontic patients with removable appliances is below the required level [2]. Another major factor is the drive to

increase efficiency through the use of skeletal support combined with fixed appliances [12], [49]. Classic laboratory-made fixed appliances consist of factory rings, screws and orthodontic wire, which, after appropriate bending, is welded or soldered to them [39]. All these elements are usually made of Cr-Ni alloys. Modern medical trends are to avoid Ni-containing metals due to the frequency of cases with manifestations of hypersensitivity to this element [21], [30]. An alternative to Cr-Ni alloys are Co-Cr alloys. They have also better corrosion resistance [8], [28], [26],

---

\* Corresponding author: Sabina Cherneva, Institute of Mechanics, Bulgarian Academy of Sciences, Acad. G. Bontchev St., bl. 4, 1113 Sofia, Bulgaria. E-mail: sabina\_cherneva@yahoo.com

Received: May 23rd, 2023

Accepted for publication: August 28th, 2023

[50] mechanical and biological properties. Elshahawy et al. [7] explained the better biological properties with the lower cytotoxicity of Cr and Mo. In addition, Huang [14] pointed out that Cr and Mo form a stable passive layer on the surface of the alloy, which reduces the possibility of ion detachment. The classic way to make Co-Cr alloy structures in dentistry is by wax modeling and casting. Wataha [46] pointed out the difficulties in this process related to casting the alloy at high temperature and the hardness of the alloy making subsequent machining of the cast structure difficult. We can add the low predictability of the final result when casting metal alloys from wax modeling, related to problems such as hollows in the structure, solidification or burning of the metal, etc. [27].

With the introduction of CAD/CAM technologies in dentistry, the working protocol of planning and manufacturing orthodontic appliances and the metal parts of prosthetic structures is completely changing [10]. Initial understandings of CAD/CAM in dentistry were associated with subtractive manufacturing methods – metal block milling [4], [48]. In this method, the mechanical properties of the material are known in advance and they do not change during the technological process. In recent years, additive manufacturing methods and the use of selective laser sintering or melting, in which the final product is made after sintering or melting metal powder, are increasingly used in dentistry [11], [38].

Van Noort defined additive manufacturing as a method for making objects from a 3D project by joining sequentially applied layers [44]. According to Webb, this technology is very economical as it involves minimal post-production waste, as unused material can be reused or recycled [47]. This technology successfully replaces a classic method in dentistry for manufacturing metal appliances, through wax modeling and metal casting [25], which is significantly more labor-intensive and time-consuming. In selective laser melting, the laser, scanning the metal powder layer by layer, heats it slightly above the melting temperature, at which fusion of the metal particles occurs [34]. In this process, the settings of the laser and the thickness of the printing layer (z-axis) are important. Tang et al. [43] believe that increasing the number of layers and the density of the laser beam leads to an increase in the density of the structure, but may worsen its accuracy.

Depending on the manufacturing parameters, samples with a different structure and, therefore, with different mechanical properties are obtained, that is why it is necessary to study the mechanical properties of the obtained samples.

The aim of this article was to evaluate the mechanical properties, elemental composition and surface characteristics of dental Co-Cr alloys intended for additive manufacturing.

## 2. Materials and methods

The investigated Co-Cr sample was 3D-printed by means of selective laser melting (SLM) method, using Wirobond® C+ alloy (BEGO Bremer Goldschlägerei, Bremen, Germany). For selective laser melting, we used a TruPrint 1000 apparatus (TRUMPF Laser- und Systemtechnik GmbH). The manufacturing parameters of the 3D-printed Co-Cr sample are collected in Table 1. According to the producer, the Wirobond® C+ chemical composition in % by weight is Co 63.9%, Cr 24.7%, W 5.4%, Mo 5.0 % and Si ≤ 1% [15].

Table 1. Manufacturing parameters of the 3D-printed Co-Cr sample

Manufacturing parameter	Value	Unit
Laser Source	Fiber laser	–
Laser power	90	W
Layer thickness	20	μm
Laser spot	55	μm
Beam speed	1100/800	–
Scan head speed	600	mm/s
Hatching step	60	μm
Oxygen level	0.44	%

A scanning electron microscope (SEM) “HIROX SH-5500P”, equipped with an integrated Energy-Dispersive X-Ray Spectroscopy (EDS) system “QUANTAX 100 Advanced” (Bruker) was used for investigation of the surface morphology and elemental composition of the 3D-printed Co-Cr sample. SEM is intended for comprehensive studies and characterization of metallic and non-metallic materials, alloys and composites at micro- and nano-levels. It consists of two modules:

- scanning electron microscope for surface topography and microstructure imaging as well as fractographic studies,
- EDS system for determining the chemical composition and distribution of metallic and non-metallic phases, inclusions, defects, coatings, etc.

The measurements were made at accelerating voltage range of 20 kV.

A “MIT500” microscope at magnifications up to 1000× was used for investigation of the microstructure of the Co-Cr sample and the sample surface was

photographed with a DV500 digital camera. The metallographic samples were poured into molds with acrylic resin. They were prepared by mechanically wet grinding the cross sections with grinding papers from P320 to P2000. Then they were mechanically polished using lubricant and diamond paste  $1/2 \mu\text{m}$ . The equipment used for preparing of the metallographic samples was Knuth-Rotor and DP-10 (Struers, Copenhagen, Denmark). The microstructure is revealed by immersing the samples in a solution of aqua regia (75 ml HCl + 25 ml HNO<sub>3</sub>).

The X-ray structural analysis of the 3D-printed Co-Cr sample was made with a Bruker D8 Advance powder X-ray diffractometer. In order to determine the qualitative and quantitative phases of analysis, we used Bruker DIFFRAC.EVA v4 program and ICDD PDF-2 (2021) comparison database with reference measurements of inorganic compounds. We calculated the crystallite size along a single line by means of the Scherrer equation and a Bruker Topas v4.2 diffraction profile analysis program.

An atomic force microscopy (AFM) was used to investigate the surface topography. NanoScope V system (Bruker Inc., Germany) operating in tapping mode in air at room temperature was used for AFM imaging. The measurements were made using silicon cantilevers (Tap 300 Al-G, Budget Sensors, Innovative Solutions Ltd., Bulgaria) with a 10 nm-thick aluminum reflex coating. Two scanning sizes ( $5 \mu\text{m} \times 5 \mu\text{m}$  and  $10 \mu\text{m} \times 10 \mu\text{m}$ ) were used and the scanning rate was 0.5 Hz. The highest possible resolution mode of the AFM ( $512 \times 512$  pixels) was used for the images, by means of the NanoScope software.

Tensile test, a three-point bending test, and nanoindentation experiments were used for investigation of mechanical properties of the 3D-printed Co-Cr sample. The tensile test was made by means of electromechanical machine Instron 1185 (UK) at an absolute deformation rate of 0.2 mm/min, following the ISO

6892-1:2019 standard [17]. The electromechanical machine Mecmesin 2, 5-i (UK) at a speed of absolute deformation of 1 mm/min was used for the three-point bending tests of Co-Cr sample. The ISO 7438:2020 [18] standard was followed for the bending tests. We made the nanoindentation experiments by means of Nanoindenter G200 (KLA Corporation, Milpitas, USA) with Berkovich tip, according to the ISO 14577 standard [16]. We used a cyclic indentation method with 5 loading-unloading cycles to find out if the properties of the samples change with depth. The method has load control with maximum load of 289 mN, peak hold time 10s, and time to load 15 s. We made 25 indentations on the surface of the investigated Co-Cr sample. The distance between the imprints was  $50 \mu\text{m}$ .

The data analysis was performed using the statistical software IBM SPSS version 28 (Chicago, IL, USA, 2021). The target variables, indentation modulus and indentation hardness, were normally distributed according to the Shapiro–Wilk test ( $p = 0.561$  for modulus;  $p = 0.818$  for hardness). The means, standard deviations (SD), minimum and maximum values were used to describe the results. The relationship between indentation modulus and indentation hardness was examined through a two-tailed Pearson- $r$  correlation analysis at a level of significance  $\alpha = 0.05$  ( $p < 0.001$ ). The plot of the residuals versus fitted values showed that homogeneity of variances (homoscedasticity) could be assumed.

## 3. Results

### 3.1. SEM results

The surface of the Co-Cr specimen at  $500\times$  and  $2000\times$  magnification, shown in Fig. 1, labeled as A

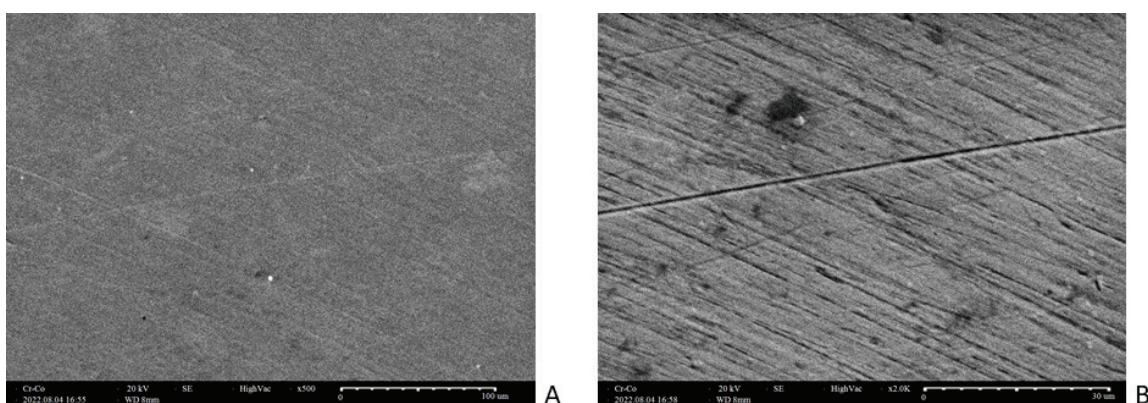


Fig. 1. SEM image of the surface of the 3D-printed Co-Cr sample: A)  $500\times$ , B)  $2000\times$

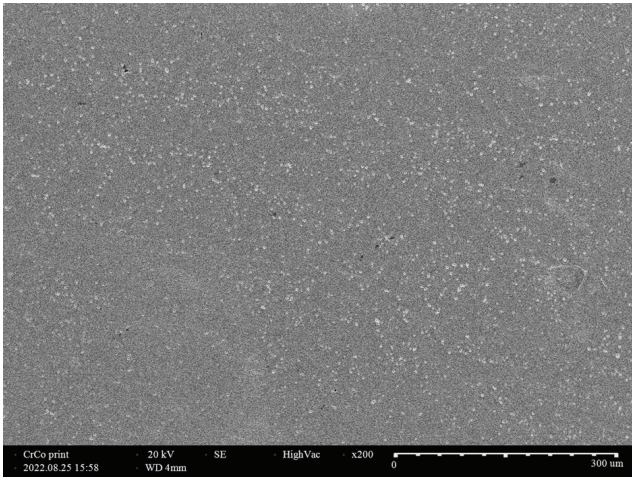


Fig. 2. SEM study inside the Co-Cr alloy specimen

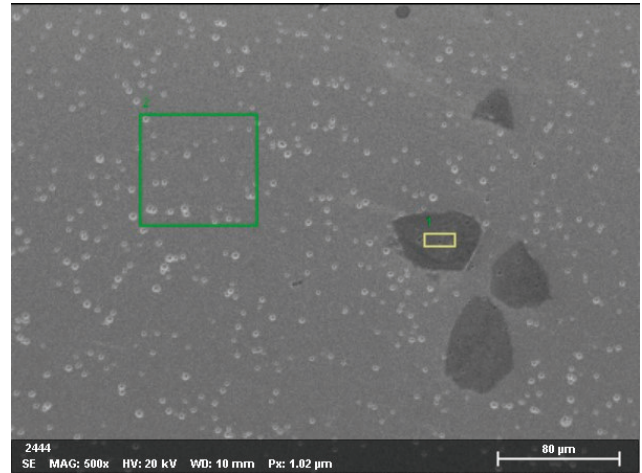


Fig. 3. SEM examination with secondary electrons inside the Co-Cr alloy specimen in zone-1 and zone-2

and B, respectively, was imaged using the scanning electron microscope. The surface of the specimen was photographed without any prior mechanical and chemical treatment. At 500 $\times$  magnification, the surface of the specimen appears homogeneous and smooth except for one or two lines caused by mechanical damage (scratches). At 2000 $\times$  magnification, thin, fine stripes were observed across the entire surface, parallel to each other with a thickness of less than 1  $\mu\text{m}$ . With a high probability, these stripes (striations) are the result of the method of obtaining the sample, through 3D-printing. The SEM study inside the Co-Cr alloy

specimen is shown in Fig. 2. Numerous small white microdots are observed, which we believe are micropores produced by selective laser melting (SLM). The high temperature gradient that occurs in the SLM manufacturing process is likely to cause stress and the formation of these micropores. In general, the structure inside the sample is dense and homogeneous.

The mass and atomic percentages of the main chemical elements involved in the Co-Cr alloy are collected in Table 2. Of interest is the study in zone-1 shown in Fig. 3, marked with a yellow rectangle, where three black structures in the form of polygons resembling

Table 2. Elemental composition in zone 1 of the sample

Element	At. no.	Netto	Mass [%]	Mass norm [%]	Atom [%]	Abs. error [%] (1 sigma)	Rel. error [%] (1 sigma)
Co	27	3281	49.74	55.04	32.23	1.66	3.35
Cr	24	2158	18.70	20.70	13.74	0.70	3.75
C	6	330	16.47	18.23	52.38	5.30	32.18
W	74	127	4.14	4.58	0.86	0.43	10.41
Mo	42	89	1.03	1.14	0.41	0.15	14.72
Si	14	27	0.28	0.31	0.38	0.09	30.38
		Sum	90.37	100.00	100.00		

Table 3. Elemental composition in zone 2 of the sample

Element	At. no.	Netto	Mass [%]	Mass norm [%]	Atom [%]	Abs. error [%] (1 sigma)	Rel. error [%] (1 sigma)
Co	27	4702	53.37	62.78	55.11	1.69	3.16
Cr	24	2988	19.56	23.01	22.90	0.69	3.52
W	74	215	6.05	7.11	2.00	0.50	8.25
C	6	77	3.35	3.94	16.96	1.88	56.24
Mo	42	160	1.81	2.13	1.15	0.20	11.07
Si	14	92	0.87	1.02	1.88	0.14	15.76
		Sum	85.01	100.00	100.00		

crystals with increased carbon content are observed. It is possible that the contamination of the sample with carbon is from the resin with which the sample was poured during the preparation of the section or during the selective laser melting process. The formation (presence) of minimal amounts of chromium and cobalt microcarbides that cannot be detected by X-ray phase analysis is also very likely.

In Table 3, the mass and atomic percentages of the main chemical elements involved in the Co-Cr alloy taken in zone-2 are shown. The EDS studies of the elements in zone-2 indicated by a green rectangle depicted in Fig. 3 correspond to the initial chemical composition of the sample. In general, zone-2 fully characterizes the structure and elemental composition of the studied sample in its entire volume.

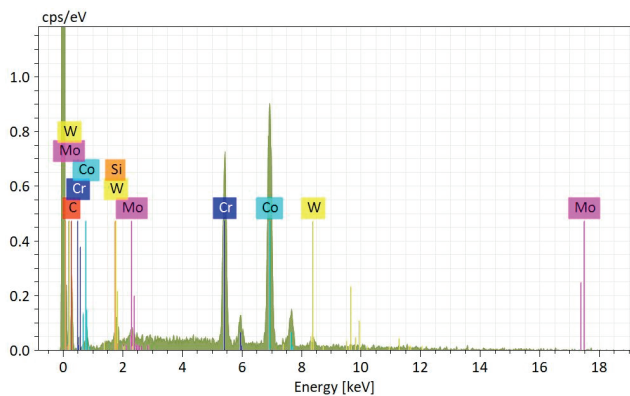


Fig. 4. The spectra of the chemical elements obtained in zone-1

The spectra shown in Figs. 4 and 5 are quite similar in elemental composition, with those in zone-2 completely matching the chemical composition of the

original sample (Wirobond<sup>®</sup> C+), and those in zone-1 having an increased carbon content.

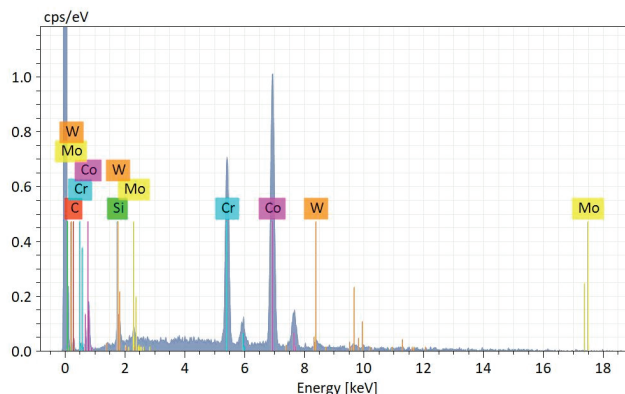


Fig. 5. The spectra of chemical elements obtained in zone-2

### 3.2. XRD results

From the X-ray structural analysis shown in Fig. 6, three phases are observed, two major and one less pronounced phase. The first phase is predominantly Chromium Cobalt ( $Co_{0.8}Cr_{0.2}$ ), the second is Cobalt Tungsten ( $Co_{0.9}W_{0.1}$ ), and the third, in the smallest amount, is very likely the intermetallic  $Co_7W_6$ , corresponding to the original composition of the sample.

### 3.3. Nanoindentation results

The experimental load-displacement curves were obtained as a result of nanoindentation experiments (Fig. 7). The indentation hardness and indentation

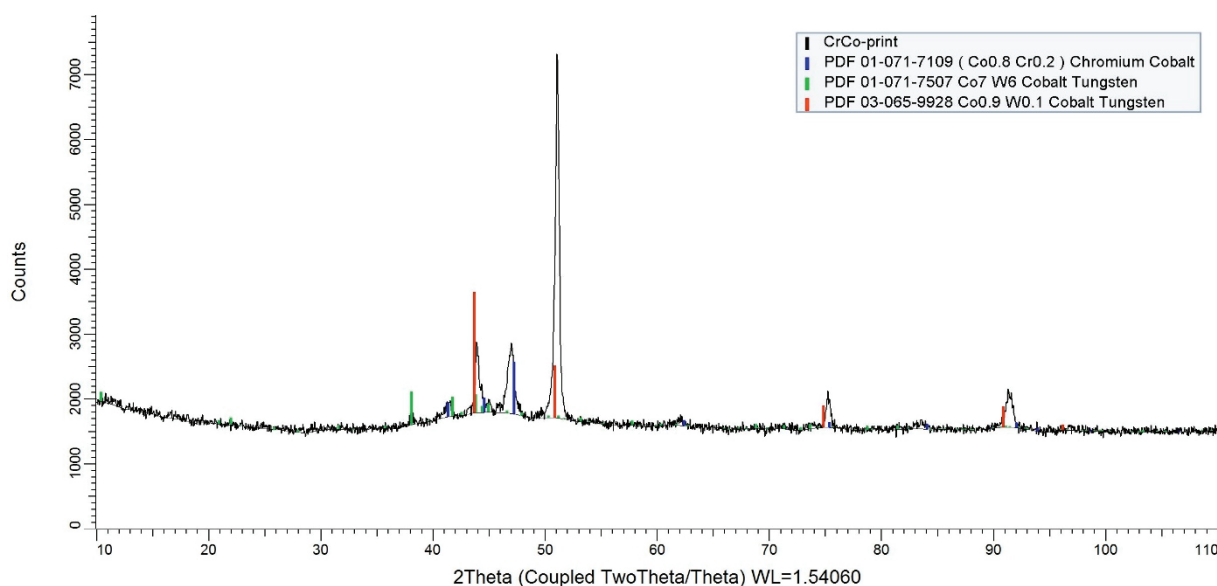


Fig. 6. Diffraction pattern of the 3D-printed Co-Cr sample

modulus of investigated 3D-printed Co-Cr sample were calculated using Oliver and Pharr method [32]. The results are presented in Figs. 8 and 9. The changes of mechanical properties in depth were investigated as well, using nanoindentation method with 5 loading-unloading cycles at 5 different loads/depths. With increasing of the depth of indentation the indentation hardness decreases and the indentation modulus is almost constant. A finer-grained and more homogeneous surface structure is observed compared to titanium

alloys obtained by 3D-printing, as well as the presence of harder phases based on tungsten and molybdenum, which leads to higher indentation hardness and indentation modulus of the studied samples compared to those of Ti6V4Al alloy [42].

### 3.4. Tensile test results

As a result of the tensile test experiments, the stress-strain curve was obtained (Fig.10).

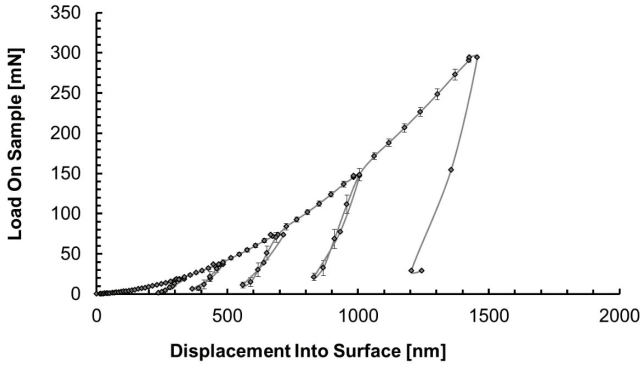


Fig. 7. Experimental load-displacement curves

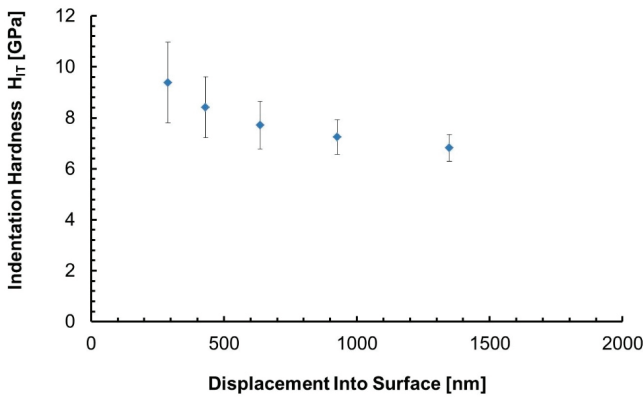


Fig. 8. Indentation hardness of investigated 3D-printed Co-Cr sample

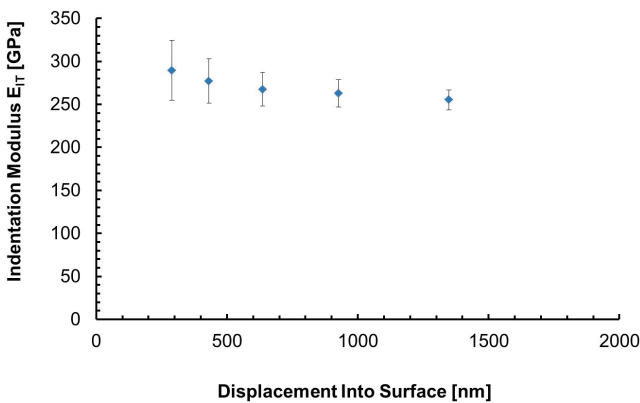


Fig. 9. Indentation modulus of investigated 3D-printed Co-Cr sample

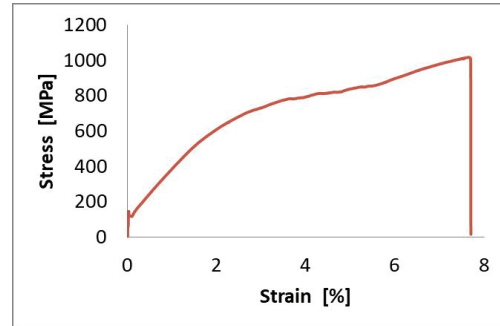


Fig. 10. Experimental stress-strain curves for the 3D-printed Co-Cr sample, obtained by means of tensile test

The observed fluctuations in the stress–strain curve of the 3D-printed Co-Cr sample (in the range of 3.0–5.4%) are due to slippage of the specimen in the grips of the machine during its loading. Therefore, the real value of the deformation at the time of failure of this test specimen is smaller. The slip estimate is slightly above 0.6%, by which value the relative deformation reported on the graph should be adjusted downward.

The fracture profile of 3D- printed Co-Cr sample (40×) after tensile test is shown in Fig. 11.

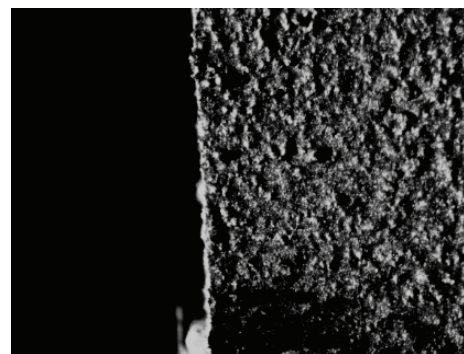


Fig. 11. Fracture profile of 3D-printed Co-Cr sample (40×) after tensile test

The presence of a straight line (Fig. 11) in the exemplarily shown area of the Co-Cr specimen speaks of an unequivocal process of brittle failure. An addi-

Table 4. The mechanical properties of the 3D-printed Co-Cr alloy, obtained by a tensile test

#	Material	$G'_{max}$	$\varepsilon (G'_{max})^1$	$G'_{yeld}$	$E'$
		[MPa]	[%]	[MPa]	[Gpa]
1	3D-printed Co-Cr	1016	7.0 <sup>2</sup>	636.5	51.8

$G'_{max}$  – the maximum tensile stress,  $\varepsilon (G'_{max})$  – the elongation at the corresponding stress, ( $G'_{yeld}$ ) – tensile stress at 0.2% relative elongation of the specimen,  $E'$  – the tensile modulus of elasticity

<sup>1</sup> The relative elongation (%) indicated in the table refers to the moment of the maximum strength value reached, and not to the moment of failure of the test body.

<sup>2</sup> The value of the indicated relative strain for the 3D-printed Co-Cr specimen is after the correction for the slip of the specimen.

tional feature of the observed areas of Fig. 11 is also the lack of surface waviness, characteristic of the cases of significant creep of the metal polycrystalline grains.

The mechanical properties of the 3D-printed Co-Cr alloy, obtained by a tensile test are shown in Table 4.

### 3.5. Three-point bending test results

The obtained results from the three-point bending test experiments of investigated 3D-printed Co-Cr sample are shown in Fig. 12. What is immediately noticeable in Fig. 12 is that at the initial moments of the load, an unstable development of the load-displacement curve is observed. However, in the initial section, the angular dependence coefficient is analogous to that observed after about 0.5 mm sag of the specimen, which is taken as the region of linear development of the load-displacement curve. The Co-Cr specimen fails to develop significant plastic deformation and fails brittle, despite the nonlinearity of the force-displacement curves.

The first impression is that there is a division of the body into at least two parts. This is characteristic

of fragile bodies. This fact completely coincides with the result of the tensile test. A closer comparison of the objects in Fig. 13 makes it possible to notice a difference in the silhouette of the upper edge of the fracture. In the test body loaded with 1 mm/min (Fig. 13A), there are traces of partial plastic deformation – the silhouette line is slightly curvy. Visibly different was the destruction of the body when it was loaded at a speed of 60 mm/min (Fig. 13B). A clearly defined straight line is a classic example of brittle failure. The results of these physico-mechanical tests are summarized in Table 5.

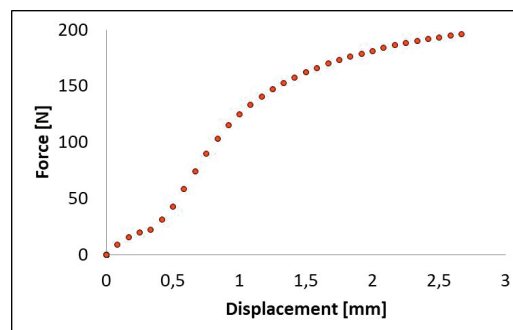


Fig. 12. Load-displacement curves, obtained by means of 3-point bending test (1 mm/min)

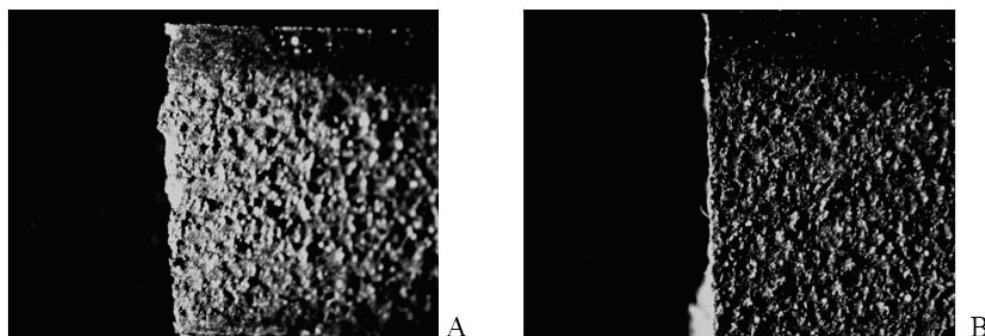


Fig. 13. Fracture profile of Co-Cr specimens after 3 point-bending test at strain rate: A) 1 mm/min, B) 60 mm/min

Table 5. Flexural strength (classical method) of the tested materials

#	Type	$G^f$	$E^f$
		[MPa]	[GPa]
1	Co-Cr SLM	1908	124
2		1891	128

$G^f$  – the maximum bending stress,  $E^f$  – flexural modulus of elasticity.

The Specimens with index “2” were tested at an indenter travel speed of 60 mm/min. The strength achieved at different loading rates may be a function of the way in which the test specimens were manufactured. Increasing speed caused a proportional decrease in recorded flexural strength of ~0.9%, a difference within statistical error.

### 3.6. AFM results

The topography and surface roughness of the 3D-printed Co-Cr samples were determined using Atomic Force Microscope (AFM) and shown in Fig. 14. On the

nanometer scale, the topography of the 3D-printed Co-Cr samples with a scanned area of  $10 \times 10 \mu\text{m}$  and a scanned area of  $5 \times 5 \mu\text{m}$  is a smooth and homogeneous. In sectional analysis of the surface and scanned area  $5 \times 5 \mu\text{m}$  for the Co-Cr sample, zones with height in the interval of  $5 \div 10 \text{ nm}$  are observed. In 3D images of 3D printed Co-Cr samples, thin, fine stripes were observed all over the surface (Fig. 15), analogous as in the SEM measurement at  $2000\times$  magnification.

### 3.7. Statistical analysis result

The descriptive statistics showed a mean value of  $254.87 \pm 11.70 \text{ GPa}$  for indentation modulus, with a minimum value of  $230.00 \text{ GPa}$  and a maximum value of  $273.00 \text{ GPa}$  (Table 6). For indentation hardness, the mean was  $6.76 \pm 0.52 \text{ GPa}$ , with individual values ranging from  $5.70 \text{ GPa}$  to  $8.10 \text{ GPa}$ .

A strong positive association was found between indentation modulus and indentation hardness with  $r = 0.535$  (95% CI: 0.210 to 0.789),  $p = 0.004$  (Fig. 16).

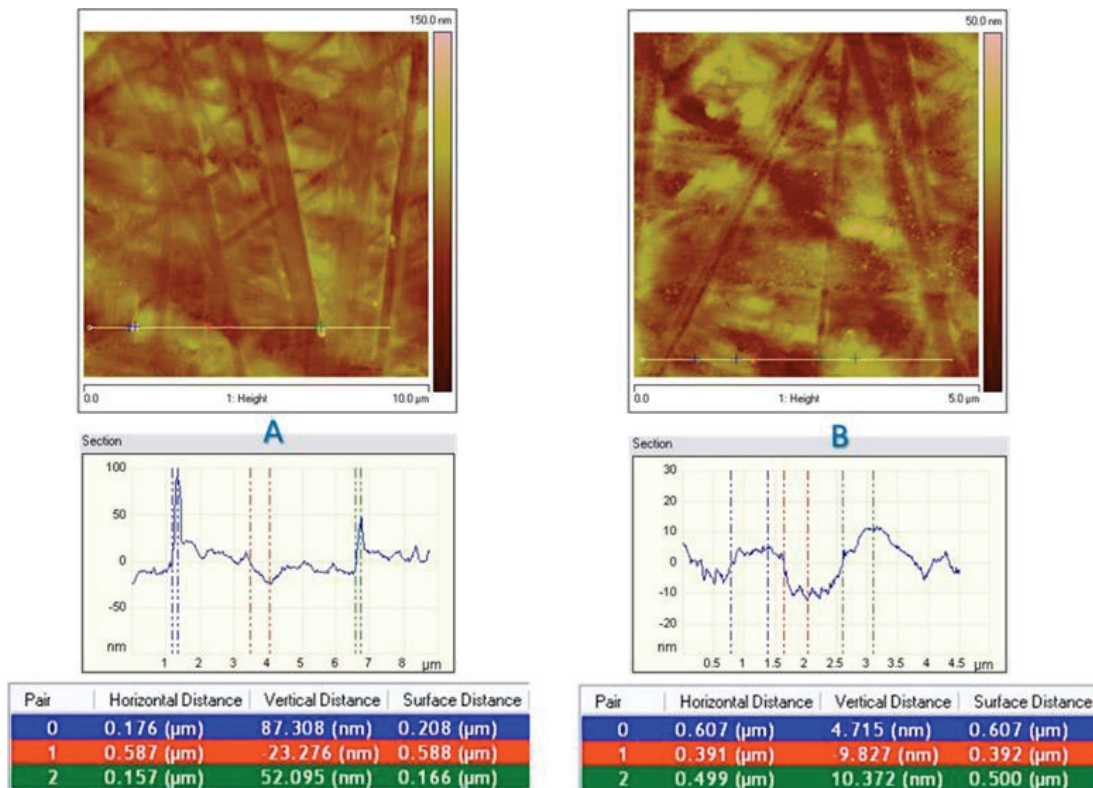


Fig. 14. AFM 2D images and section analysis of the surface of the 3D-printed Co-Cr sample: A)  $10 \times 10 \mu\text{m}$ , B)  $5 \times 5 \mu\text{m}$

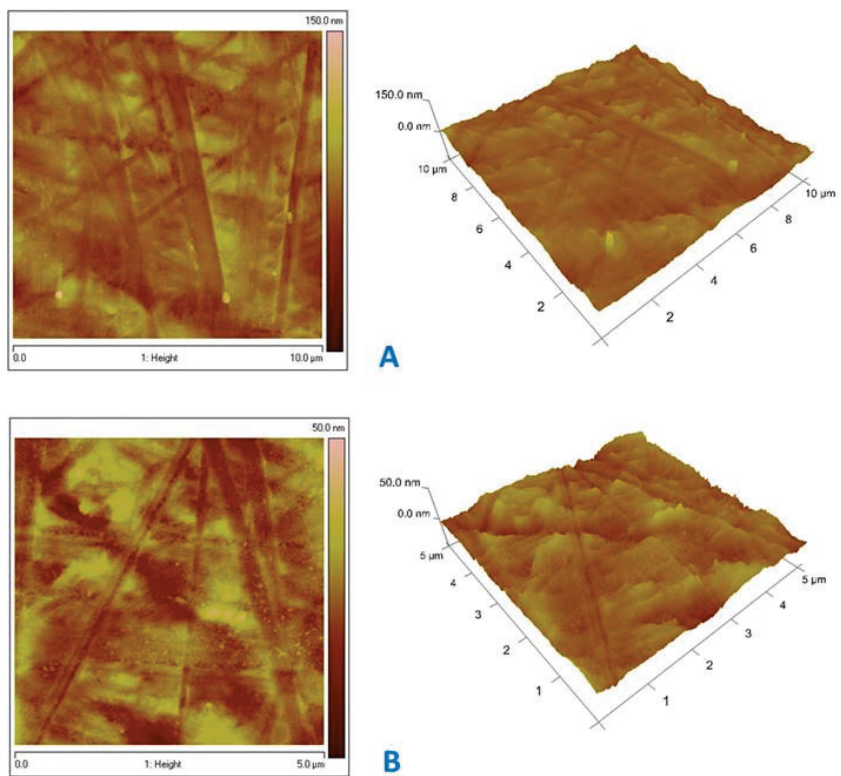


Fig. 15. AFM 2D and 3D images of the surface of the 3D-printed Co-Cr sample: A) 10 × 10 μm, B) 5 × 5 μm

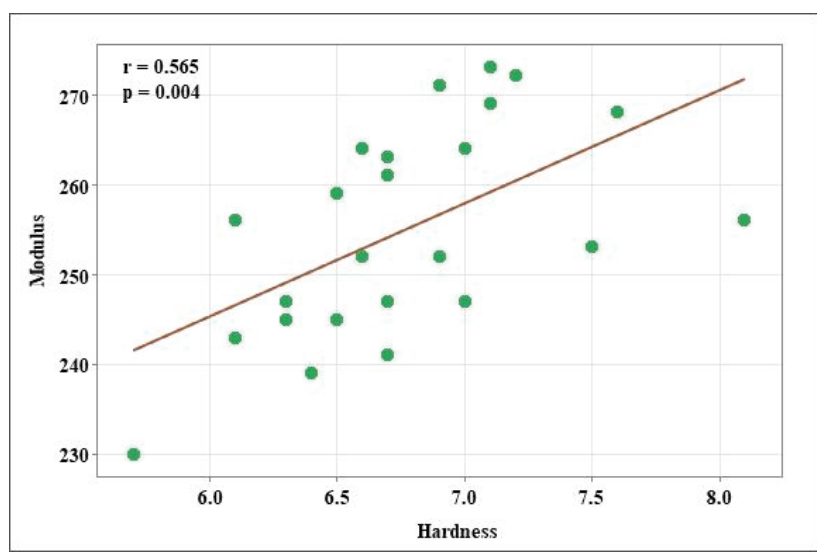


Fig. 16. Scatterplot of indentation modulus versus indentation hardness

Table 6. Descriptive statistics for indentation modulus and indentation hardness at maximum load in the 3D printed Co-Cr sample

Parameter	Mean	SD	Minimum	Maximum
Indentation modulus (n = 25)	254.87	11.70	230.00	273.00
Indentation hardness (n = 25)	6.76	0.52	5.70	8.10

### 4. Discussion

Co-Cr alloys have been recently used widely in orthopedics and dentistry because of its biocompatibility, lower cost, good mechanical properties, wear and corrosion resistance as well as less number of allergic reactions compared to nickel containing alloys. Co-Cr alloys are used not only in the medicine,

but also for producing of industrial gas turbines, fuel nozzles and jet engines. The advantages of the SLM process, which we used for production of our Co-Cr alloy are possibility of production of details with complex shape, highly precise patient-specific implants, minimum post-processing and assembly requirements, better quality of finished products and comparable mechanical load performance of the fabricated parts with the traditional production technology, metallic implants can be printed just-in-time, reduce inventory costs [29]. Although many investigations of different Co-Cr alloys have been made [1], [3], [5], [6], [13], the different technological regimes and parameters of the production process, as well as characteristics of starting powders, lead to different microstructure of the obtained alloy [22], [37], which is one of the reasons for different mechanical properties, obtained by us and some of the aforementioned authors.

The results from our nanoindentation experiments show that with increasing of the depth of indentation the indentation hardness decreases. One possible reason for this difference of properties in depth can be the thick solid dense oxide  $\text{Cr}_2\text{O}_3$  film, which usually is formed on the surface of the Co-Cr sample [13], as well as layer-by-layer production process. The obtained results for indentation hardness and indentation modulus are in good agreement with these, obtained from Fu [9], Videršćak [45] and Kim [20]. We obtained higher values of indentation hardness, tensile strength, yield strength and flexural strength of 3D printed by selective laser melting Co-Cr alloys in comparison with cast Co-Cr [23], [31] and Cr-Ni alloys [24], [33], [36]. The influence of two different strain rates (1 mm/min and 60 mm/min) on the flexural strength was investigated as well. It was found that increasing speed caused a proportional decrease in recorded flexural strength of  $\sim 0.9\%$ . The strength achieved at different loading rates may be a function of the way in which the test specimens were manufactured.

The SEM analysis shows a uniform and fine structure over the entire examined surface, which contributes to the unchanged characteristics and properties of the 3D-printed sample over time. Three predominant phases  $\text{Co}_{0.9}\text{W}_{0.1}$  – hexagonal,  $\text{Cr}_{0.8}\text{Co}_{0.2}$  – cubic and  $\text{Cr}_7\text{W}_6$  – rhombohedral have been obtained. These phases determine the high hardness and, respectively, the high wear resistance of the studied material obtained by 3D printing. The AFM analysis confirm homogenous surface with low values of the roughness in the nanometric scale. Our results also coincide with the research of Saini, [40], according to whom the Co-Cr alloys produced by SLM possess the dense, compact and homogeneous microstructure, which is superior to

the cast Co-Cr alloys. This is also the reason why we believe that for the purpose of making orthodontic appliances, the laser melting technology gives better results than the direct metal laser sintering (DMLS) technology, where complete melting and fusion of the metal particles does not occur. In this technology, the laser settings are selected to heat the metal powder to a temperature just below the metal's melting point. In this, bridges are formed between the metal particles, without complete fusion [41]. The result is a more porous structure with weaker mechanical properties [19], [43]. This would have its advantages in the fabrication of metal-ceramic frameworks, as the porous structure of the metal favors bonding with the opacer, but not for orthodontic or cast prosthesis purposes.

## 5. Conclusions

Based on the results of our research, we can claim that the laser-sintered Co-Cr alloy can fully replace the cast Co-Cr alloy in dentistry. The simplified work protocol associated with digital planning and additive manufacturing of structures guarantee high precision of the final product. We believe that this, combined with the good mechanical properties of the laser-sintered Co-Cr alloy, will make this method fundamental in the fabrication of metal removable and non-removable structures in dentistry.

## References

- [1] AL JABBARI Y.S., KOUTSOUKIS T., BARMAGADAKI X., ZINELIS S., *Metallurgical and interfacial characterization of PFM Co-Cr dental alloys fabricated via casting, milling or selective laser melting*, Dent. Mater., 2014, 30, e79-e88.
- [2] AL-MOGHRABI D., SALAZAR F., PANDIS N., FLEMING P., *Compliance with removable orthodontic appliances and adjuncts: A systematic review and meta-analysis*, Am. J. Orthod. Dentofacial. Orthop., 2017, 152, 17–32.
- [3] BARAZANCHI A., *Evaluation of 3D Printed and Soft Milled Cobalt Chromium Alloy for Prosthodontic Applications*, PhD Thesis, University of Otago, New Zealand, 2018.
- [4] ÇAKMAK G., DONMEZ M.B., CUELLAR A.R., KAHVECI Ç., SCHIMMEL M., YILMAZ B., *Additive or subtractive manufacturing of crown patterns used for pressing or casting: A true-ness analysis*, J. Dent., 2022, 124, 104221.
- [5] DIKOVA T., *Properties of Co-Cr Dental Alloys Fabricated Using Additive Technologies*, Chapter 5 in book "Biomaterials in Regenerative Medicine", InTech, 2018, 141–159.
- [6] DOLGOV N.A., DIKOVA T., DZHENDOV D., PAVLOVA D., SIMOV M., *Mechanical properties of dental Co-Cr alloys fabricated via casting and selective laser melting*, Scientific Proceedings II International Scientific-Technical Conference "Innovations in Engineering", 2016, 29–33.

- [7] EL SHAHAWY W.M., WATANABE I., KRAMER P., *In vitro cytotoxicity evaluation of elemental ions released from different prosthodontic materials*, Dent. Mater., 2009, 25, 1551–1555.
- [8] FARIA A.C., ROSA A.L., RODRIGUES R.C., RIBEIRO R.F., *In vitro cytotoxicity of dental alloys and cpTi obtained by casting*, J. Biomed. Mater. Res. B Appl. Biomater., 2008, 85, 504–508.
- [9] FU W., LIU S., JIAO J., XIE Z., HUANG X., LU Y., LIU H., HU S., ZUO E., KOU N., MA G., *Wear Resistance and Biocompatibility of Co-Cr Dental Alloys Fabricated with CAST and SLM Techniques*, Mater., 2022, 15, 3263.
- [10] GHISLANZONI L., NEGRINI S., *Digital Lab Appliances: The Time Has Come*, J. Clin. Orthod., 2020, 54, 562–569.
- [11] GRAF S., *Clinical guidelines for direct printed metal orthodontic appliances*, Semin. Orthod., 2018, 24, 461–469.
- [12] GRAF S., VASUDAVAN S., WILMES B., *CAD/CAM Metallic Printing of a Skeletally Anchored Upper Molar Distalizer*, J. Clin. Orthod., 2020, 54, 140–150.
- [13] HONG J.H., YEOH F.Y., *Mechanical properties and corrosion resistance of cobalt-chrome alloy fabricated using additive manufacturing*, Mater. Today. Proc., 2020, 29, 196–201.
- [14] HUANG H.H., *Effect of chemical composition on the corrosion behavior of Ni-Cr-Mo dental casting alloys*, J. Biomed. Mater. Res., 2002, 60, 458–465.
- [15] <https://www.bego.com/index.php?id=156&L=624>
- [16] ISO 14577-1:2015. *Metallic materials – Instrumented indentation test for hardness and materials parameters. Part 1: Test method*
- [17] ISO 6892-1:2019. *Metallic materials – Tensile testing. Part 1: Method of test at room temperature*
- [18] ISO 7438:2020(en). *Metallic materials – Bend test*
- [19] KHAING M., FUH J., LU L., *Direct metal laser sintering for rapid tooling: processing and characterisation of EOS parts*, J. Mat. Proc. Techn., 2001, 113, 269–272.
- [20] KIM H.R., JANG S.-H., KIM Y.K., SON J.S., MIN B.K., KIM K.-H., KWON T.-Y., *Microstructures and Mechanical Properties of Co-Cr Dental Alloys Fabricated by Three CAD/CAM-Based Processing Techniques*, Mater., 2016, 9, 596.
- [21] KOLOKITHAA O., CHATZISTAVROU E., *A Severe Reaction to Ni-Containing Orthodontic Appliances*, Angle Orthod., 2009, 79, 186–192.
- [22] KONIECZNY B., SZCZESIO-WŁODARCZYK A., SOKOŁOWSKI J., BOCIONG K., *Challenges of Co-Cr Alloy Additive Manufacturing Methods in Dentistry – The Current State of Knowledge (Systematic Review)*, Mater., 2020, 13, 3524.
- [23] KOUTSOUKIS T., ZINELIS S., ELIADES G., AL-WAZZAN K., RIFAIY M.A., AL JABBARI Y.S., *Selective Laser Melting Technique of Co-Cr Dental Alloys: A Review of Structure and Properties and Comparative Analysis with Other Available Techniques*, J. Prosthodont., 2015, 24, 303–312.
- [24] LIN H.-Y., BOWERS B., WOLAN J., CAI Z., BUMGARDNER J., *Metallurgical, surface, and corrosion analysis of Ni-Cr dental casting alloys before and after porcelain firing*, Dent. Mater., 2008, 24, 378–385.
- [25] LIU C., QIAO X., ZHANG S., MA W., WANG W., GE X., HU X., KANG W., LU H., *Banded versus modified appliances for anchorage during maxillary protraction*, J. Orofac. Orthop., 2020, 81, 172–182.
- [26] LOCH J., ŁUKASZCZYK A., AUGUSTYN-PIENIAŻEK J., KRAWIEC H., *Electrochemical Behaviour of Co-Cr and Ni-Cr Dental Alloys*, SSP, 2015, 227, 451–454.
- [27] MAJERIC D., LAZIC V., MAJERIC P., MARKOVIC A., RUDOLF R., *Investigation of CoCr Dental Alloy: Example from a Casting Workflow Standpoint*, Cryst., 2021, 11, 849.
- [28] MERCIĘCA S., CONTI M., BUHAGIAR J., CAMILLERI J., *Assessment of corrosion resistance of cast cobalt- and nickel-chromium dental alloys in acidic environments*, J. Appl. Biomater. Funct. Mat., 2018, 16, 47–54.
- [29] MUNIR K., BIESIEKIERSKI A., WEN C., LI Y., *Selective laser melting in biomedical manufacturing* (Chapter 7), [in:] *Metallic Biomaterials Processing and Medical Device Manufacturing*, Woodhead Publishing, 2020, 235–269.
- [30] NOBLE J., AHING S., KARAIKOS E., WILTSHIRE W., *Nickel allergy and orthodontics, a review and report of two cases*, Br. Dent. J., 2008, 204, 297–300.
- [31] ØILO M., NESSE H., LUNDBERG O., GJERDET N., *Mechanical properties of cobalt-chromium 3-unit fixed dental prostheses fabricated by casting, milling, and additive manufacturing*, J. Prosthet. Dent., 2018, 120, 156.e1–156.e7.
- [32] OLIVER W.C., PHARR G.M., *An improved technique for determining hardness and elastic modulus using load and displacement sensing indentation experiments*, J. Mater. Res., 1992, 7, 1564–1583.
- [33] OLIVIERI K., NEISSER M., DE SOUZA P., BOTTINO M., *Mechanical properties and micro structural analysis of a NiCr alloy cast under different temperatures*, Braz. J. Oral. Sci., 2004, 3, 414–419.
- [34] PAOLETTI I., CECCON L., *The Evolution of 3D Printing in AEC: From Experimental to Consolidated Techniques* (Chapter 3), [in:] “3D Printing”, InTechopen, 2018.
- [35] PAPADOPOULOS M., *Orthodontic Treatment of the Class II Noncompliant Patient*, Mosby Ltd, 2006
- [36] PIMENTA A., DINIZ M., PACIORNIK S., SAMPAIO C., DE MIRANDA M., PAOLUCCI-PIMENTA J., *Mechanical and microstructural properties of a nickel-chromium alloy after casting process*, RSBO, 2012, 9, 17–24.
- [37] PRESOTTO A., CORDEIRO J., PRESOTTO J., RANGEL E., DA CRUZ N., LANDERS R., BARÃO V., MESQUITA M., *Feasibility of 3D printed Co-Cr alloy for dental prostheses applications*, J. Alloys Compd, 2021, 862, 2021, 158171.
- [38] REVILLA-LEON M., MEYER M., OZCAN M., *Metal additive manufacturing technologies: literature review of current status and prosthodontic applications*, Int. J. Comput. Dent., 2019, 22, 55–67.
- [39] RODRIGUES A., MONINI A., GANDINI L., SANTOS-PINTO A., *Rapid palatal expansion: a comparison of two appliances*, Braz. Oral. Res., 2012, 26, 242–248.
- [40] SAINI J.S., DOWLING L., TRIMBLE D., SINGH D., *Mechanical Properties of Selective Laser Melted CoCr Alloys: A Review*, J. Mater. Eng. Perform., 2021, 30, 8700–8714.
- [41] SHEELA U., USHA P., JOSEPH M., MELO J., NAIR S., TRIPATHI A., *3D printing in dental implants* (Chapter 7), [in:] D. Thomas, D. Singh, *3D Printing in Medicine and Surgery*, Woodhead Publishing Series in Biomaterials, 2021.
- [42] SURESH S., SUN C., TEKUMALLA S., ROSA V., MUI S., NAI L., WONG R., *Mechanical properties and in vitro cytocompatibility of dense and porous Ti-6Al-4V ELI manufactured by selective laser melting technology for biomedical applications*, J. Mech. Behav. Biomed. Mater., 2021, 123, 104712.
- [43] TANG Y., LOH H., WONG Y., FUH J., LU L., WANG X., *Direct laser sintering of a copper-based alloy for creating three-dimensional metal parts*, J. Mat. Proc. Techn., 2003, 140, 368–372.
- [44] VAN NOORT R., *The future of dental devices is digital*, Dent. Mat., 2012, 28, 3–12.
- [45] VIDERŠČAK D., SCHAUPERL Z., ŠOLIĆ S., ČATIĆ A., GODEC M., KOCIJAN A., PAULIN I., DONIK Č., *Additively Manufactured*

- Commercial Co-Cr Dental Alloys: Comparison of Microstructure and Mechanical Properties*, Mater., 2021, 14, 7350.
- [46] WATAHA J.C., *Alloys for prosthodontic restorations*, J. Prosthet. Dent., 2002, 87, 351–363.
- [47] WEBB P., *A review of rapid prototyping (RP) techniques in the medical and biomedical sector*, J. Med. Eng. Techn., 2000, 24, 149–153.
- [48] WILLER J., ROSSBACH A., WEBER H.P., *Computer-assisted milling of dental restorations using a new CAD/CAM data acquisition system*, J. Prosthet. Dent., 1998, 80, 346–353.
- [49] WILMES B., DE GABRIELE R., DALLATANA G., TARRAF N., LUDWIG B., *“Bone first” principle with CAD/CAM insertion guides for mini-implant-assisted rapid palatal expansion*, J. Clin. Orthod., 2022, 56, 158–166.
- [50] ZHIHONG C., YEZHEN L., ZHIYUAN G., ZHONGQIAO Y., XIAOXUE L., YIFENG R., WEIKUN F., JILIANG H., *Comparison of the cytogenotoxicity induced by five different dental alloys using four in vitro assays*, Dent. Mater. J., 2011, 30, 861–868.